

Soft Matter

Accepted Manuscript



This is an *Accepted Manuscript*, which has been through the Royal Society of Chemistry peer review process and has been accepted for publication.

Accepted Manuscripts are published online shortly after acceptance, before technical editing, formatting and proof reading. Using this free service, authors can make their results available to the community, in citable form, before we publish the edited article. We will replace this *Accepted Manuscript* with the edited and formatted *Advance Article* as soon as it is available.

You can find more information about *Accepted Manuscripts* in the [Information for Authors](#).

Please note that technical editing may introduce minor changes to the text and/or graphics, which may alter content. The journal's standard [Terms & Conditions](#) and the [Ethical guidelines](#) still apply. In no event shall the Royal Society of Chemistry be held responsible for any errors or omissions in this *Accepted Manuscript* or any consequences arising from the use of any information it contains.

The effect of guanidinium functionalization on the structural properties and anion affinity of polyelectrolyte multilayers†

Zheng Cao, ‡^{ab} Pavlo I. Gordiichuk,^c Katja Loos,^c Ernst J.R. Sudhölter,^a Louis C.P.M. de Smet*^a

^a *Organic Materials and Interfaces, Department of Chemical Engineering, Delft University of Technology, Julianalaan 136, 2628 BL Delft, The Netherlands. Email:*

l.c.p.m.desmet@tudelft.nl

^b *Wetsus, centre of excellence for sustainable water technology, Oostergoweg 9, 8911 MA Leeuwarden, The Netherlands*

^c *Zernike Institute for Advanced Materials, University of Groningen, Nijenborgh 4, 9747 AG Groningen, The Netherlands*

† Electronic supplementary information (ESI) available: ¹H NMR spectra and FT-IR spectra of PAH, PAH-Gu and guanidineacetic acid, Voigt model details, control QCM-D experiments, RAIR spectra of PSS/PAH-Gu PEMs and reference FT-IR spectra of the salts used, as well as tables with a summary of the Sauerbrey calculations and ion properties. See DOI: ...”

‡ Current address: School of Materials Science and Engineering, Changzhou University, China

Keywords: polyelectrolyte multilayers, guanidinium groups, anions, interactions, QCM-D

Abstract (196 words):

Poly(allylamine hydrochloride) (PAH) is chemically functionalized with guanidinium (Gu) moieties in water at room temperature. The resulting PAH-Gu is used to prepare polyelectrolyte multilayers (PEMs) with poly(sodium 4-styrene sulfonate) (PSS) via layer-by-layer deposition. The polyelectrolyte (PE) adsorption processes are monitored real-time by optical reflectometry and a quartz crystal microbalance with dissipation monitoring (QCM-D). Compared to the reference PSS/PAH PEMs, the PSS/PAH-Gu PEMs show a lower amount of deposited PE materials, a lower wet thickness, a higher stability at alkaline conditions and a higher rigidity. These differences are rationalized by the additional Gu-SO₃⁻ interactions, also affecting the conformation of the PE chains in the PEM. The interactions between the PEMs and various sodium salts (NaCl, NaNO₃, Na₂SO₄ and NaH₂PO₄) are also monitored using QCM-D. From the changes in the frequency, dissipation responses and supportive Reflection Absorption Infrared Spectroscopy it is concluded that Gu-functionalized

PEMs absorb more H_2PO_4^- compared to the Gu-free reference PEMs. This can be understood by strong interactions between Gu and H_2PO_4^- , the differences in the anion hydration energy and the anion valency. It is anticipated that compounds like the presented Gu-functionalized PE may facilitate the further development of H_2PO_4^- sensors and ion separation/recovery systems.

1 Introduction

Polyelectrolyte multilayers (PEMs) are a versatile type of ultrathin films, which are fabricated via layer-by-layer (LbL) assembly of positively and negatively charged polymers.¹⁻³ PEMs are a very attractive type of building block due to their easy fabrication, the ability to control the layer thickness at the nanometer level and the possibility to embed various functionalities. They have found a large variety of applications, including the preparation of nanocontainers for drug encapsulation and controlled release,⁴ nanoreactors for the synthesis of core-shell nanoparticles⁵ and antimicrobial⁶ or anticorrosion⁷ coatings. Also PEMs have been used in the fields of catalysis,⁸ sensor systems^{9,10} and membrane cleaning¹¹ and membranes for the separation purposes, including the separation of ions.¹²⁻¹⁶

The ability of PEMs to separate ions is largely based on ion size and charge selectivity, but also ionophores have been applied in the preparation of PEMs to improve the separation behaviour. Typically, one of the two oppositely charged polyelectrolytes is replaced by charged macrocyclic compounds with ion-selective properties.¹⁷ A better understanding of the interactions between (functionalized) PEMs and various ion species and its optimization are becoming increasingly important, not only for developing ion-selective materials for separation and purification purposes,¹⁸ but also for potential applications in the field of ion detection.¹⁹

A large number of studies addresses the main factors affecting the PEM assembly, the stability²⁰ and the swelling properties.²¹ These include pH,^{22,23} salt species²⁴⁻²⁶ and ionic strength,²⁷ which can all be changed during and after the multilayer build-up. In addition, ion exchange processes between supporting solutions and multilayers have been studied.²⁸⁻²⁹ For example, Salomäki *et al.* investigated a specific anion effect in swelling of poly(sodium 4-styrene sulfonate)/poly(diallyldimethylammonium chloride) (PSS/PDADMA) multilayers.²¹ More recently, Zahn *et al.* investigated ion and water exchange processes in $\text{Fe}(\text{CN})_6^{4-}$ -containing poly(L-gluamic acid)/poly(allylamine) hydrochloride PGA/PAH multilayers and observed that the swelling properties of the multilayer can be related to its interactions with different hydrated counter ions.²⁸ The results from these studies are highly relevant for the design and preparation of PEMs showing selective anion binding, a subject hardly studied so far.

Poly(allylamine hydrochloride) (PAH) is a linear, cationic polyelectrolyte commonly used in the preparation of PEMs. The side amino groups of PAH can be easily modified with compound containing carboxyl groups to form amide bonds. Recently our group presented a versatile PEM-based biosensing platform with biotinylated PAH as one of the building blocks³⁰ and we attached fluorophores to PAH for staining purposes.³¹ In the current study we modified PAH with guanidine acetic acid (GAA). Guanidinium (Gu) units can be used for the selective binding of oxoanions such as sulfates and (pyro)phosphates due to strong electrostatic and hydrogen-bond interactions.³²⁻³⁴ The guanidinium moiety adopts a unique planar Y-shaped configuration and remains protonated over a wide pH range ($\text{p}K_a \sim 13$).^{33,35} The aim of the current work is to study the effect of guanidinium functionalization on the structural and ion affinity properties of PEMs with a strong focus on H_2PO_4^- . To this end, the new functional polyelectrolyte (PAH-Gu) was used for the building up of PEMs. The LbL process and the stability of the resulting multilayers were investigated by two different surface techniques: Quartz Crystal Microbalance with Dissipation monitoring (QCM-D) and optical

reflectometry. With QCM-D, the real-time recorded frequency and dissipation shifts can provide information on (changes in) the mass and the viscoelastic properties of adsorbed layers on the crystal surfaces of QCM sensors. It has been used extensively for studying the conformation of polymer chains at interfaces,^{23,36,37} protein adsorption,³⁸ polysaccharide-lipid complex formation,³⁹ viscoelasticity of hydrogel thin films,⁴⁰⁻⁴² build-up and swelling of PEMs.^{29,43,44} Interestingly, both QCM and optical reflectometry are real-time techniques. However, there is a crucial difference: QCM-D also measures the mass of mechanically (dynamically) coupled water, while the optical mass does not contain a contribution from the solvent. Hence, by combining these two different techniques, detailed information about the structural properties of the layers can be obtained. In the final section, the thus-obtained functionalized polyelectrolyte thin films were investigated by QCM-D for their interactions with aqueous solutions containing different anions.

2 Experimental section

2.1 Chemicals and materials

Poly(allylamine hydrochloride) (PAH, average M_w ~15,000), poly(sodium 4-styrene sulfonate) (PSS, average M_w ~70,000), polyethylenimine (PEI, branched, average M_w 25,000), guanidine acetic acid (GAA, 99%), N-hydroxysuccinimide (NHS, 98%), N-(3-dimethylaminopropyl)-N'-ethylcarbodiimide hydrochloride (EDC, commercial grade) were purchased from Sigma-Aldrich and used as received. Sodium chloride (NaCl, p.a., 99.8%, Sigma-Aldrich), sodium sulfate (Na_2SO_4 , p.a. anhydrous, 99%, Fluka), sodium nitrate (NaNO_3 , p.a., Merck), sodium phosphate monobasic monohydrate ($\text{NaH}_2\text{PO}_4 \cdot \text{H}_2\text{O}$, p.a., Acros Organics) were used.

QCM sensors covered with gold (QSX301) coatings were purchased from Q-sense. Silicon wafers (p type, 0.001-0.003 Ohm.cm) were purchased from Sil'tronix S.T (France). A

SiO₂ layer of 50 nm in thickness was formed by thermal oxidation for 100 min at 1000 °C. Milli-Q water was freshly purified in a Millipore RiOs 5 reverse osmosis system.

2.2 Synthesis of functionalized PAH

A series of PAH derivatives (PAH-Gu) were prepared using EDC/NHS linking chemistry⁴⁵ to conjugate guanidine acetic acid with PAH (Scheme 1). We synthesized three PAH-Gu polyelectrolytes with different degrees of substitution by changing the molar feed ratio of the monomeric allylamine hydrochloride (AH) and GAA according to: 10:1, 10:2, 10:3. Briefly, for the 10:2 ratio case, 0.200 g of PAH (2.140 mmol of AH), 0.050 g of GAA (0.428 mmol), 0.410 g of EDC (2.139 mmol) and 0.246 g of NHS (2.139 mmol) were dissolved in 20 cm³ of Milli-Q water and allowed to react at room temperature for 70 hours. The unreacted guanidine acetic acid, EDC and NHS were separated by dialysis (dialysis tubing cellulose membrane, molecular weight cut off 14,000, Sigma-Aldrich) against Milli-Q water for 2 days during which the outer solution was refreshed every 12 hours. Finally, the water was removed by freeze drying and the functionalized polyelectrolyte was obtained as a white powder. The use of the three different molar feed ratios yielded in three different batches of PAH-Gu: #1, #2 and #3, respectively. In the rest of this study PAH-Gu refers to PAH-Gu #2 unless otherwise stated. The products were characterized with FT-IR and ¹H NMR confirming the attachment and determining the degree of substitution (DS) of the Gu functionalities onto the PAH backbone.

2.3 Preparation of aqueous polyelectrolyte and salt solutions

A NaCl solution with a concentration of 0.15 M at pH 5.5 was prepared by adding an appropriate amount of NaCl to Milli-Q water, followed by the adjustment of pH with HCl solution using a pH meter (827 pH lab, Metrohm Swiss). This NaCl solution was used as the supporting electrolyte solution in all experiments involving the preparation of polyelectrolyte

solutions and the build-up of polyelectrolyte multilayers. Each polyelectrolyte solution was prepared by adding this NaCl solution to the required amount of polymers (50 mg dm⁻³ for PEI and 22 mg dm⁻³ for all other PEs). As a glass electrode cannot be used to measure the pH of the resulting polymer solution (due to the interference by adsorption of polyelectrolytes to the glass electrode surface), the pH was checked using pH indicator paper. In the cases of PSS, PAH and PAH-Gu the pH did not change upon the addition of the polymers, so these solution were at 0.15 M and pH 5.5. In the case of PEI the pH increased to ~9. The pH was not adjusted after the addition of the polymer. Aqueous solutions of 10 mM of the investigated sodium salts, *i.e.* NaCl, NaNO₃, Na₂SO₄ and NaH₂PO₄ were made by adding Milli-Q water to the appropriate amount of salt.

2.4 Characterization of PAH-Gu

¹H NMR spectra of the PAH-Gu polymers were recorded using a Bruker AVANCE 400 NMR spectrometer with D₂O as solvent. FT-IR spectra of the PAH-Gu derivatives were obtained with a Nicolet 8700 FT-IR Spectrometer using the KBr pellet technique. The spectra were recorded over a range of 4000-400 cm⁻¹ at a resolution of 4 cm⁻¹.

2.5 Characterization of the PEMs

The real-time adsorption of polyelectrolytes from solutions onto silica surfaces to build PEI(PSS/PAH)₅ and PEI(PSS/PAH-Gu)₅ was first studied by fixed-angle, stagnation point optical reflectometry (briefly: optical reflectometry).⁴⁶ Briefly, in this technique, the reflected intensities I_p and I_s for parallel and perpendicularly polarized light are combined to an output signal defined as $S = I_p / I_s$. This output signal changes upon the adsorption of materials onto the surface and hence it is common to use the relative output signal $(S - S_0) / S_0$, where S_0 corresponds to the output signal before adsorption. The relative output signal is related to the adsorbed amount Γ (mg m⁻²) as follows:

$$\Gamma = \frac{S-S_0}{S_0} \frac{1}{A_s} = \frac{\Delta S}{S_0} \frac{1}{A_s} \quad (1)$$

where A_s is the so-called sensitivity factor, which can be determined by several experimental factors: the thickness and refractive index of the substrate, the refractive index increment of the polymer solution (dn/dc) and the refractive index of the adsorbed layer (n_{ads}).²⁰ In our case $1/A_s$, also known as the Q-factor, for the first polyelectrolyte layer equals 23.71 mg m^{-2} as calculated with the software program Prof. Huygens, version 1.2c (Dullware Software), using a value of $0.176 \text{ cm}^3 \text{ g}^{-1}$ for the dn/dc of PEI as reported in literature.⁴⁷ Standard errors bars were calculated from two independent experiments.

The real-time build-up of PEI(PSS/PAH)₆ and PEI(PSS/PAH-Gu)₆ polyelectrolyte multilayers on gold surfaces of QCM sensors was also measured using a Q-sense E4 quartz crystal microbalance with dissipation monitoring (QCM-D, QSENSE, Västra Frölunda, Sweden) in a liquid medium at 25 °C. The QCM sensor is an AT-cut quartz crystal (fundamental resonant frequency $f_0 = 5 \text{ MHz}$) covered with gold electrodes (100 nm thickness) on both surfaces. The cleaning protocols of the QCM sensor surfaces were carried out as described in literature.³⁹ The resonance characteristics of the unmodified QCM sensors in the polymer-free solution of 0.15 M NaCl at pH 5.5 were first recorded as the base line. Then the aqueous polyelectrolyte solutions were pumped through the QCM-D flow cells at a flow rate of $50 \text{ } \mu\text{L min}^{-1}$. The Au-coated QCM sensors were deposited with PEI as the first initial layer,²⁵ followed by the alternate and sequential deposition of polyanions and polycations. After the build-up of polyelectrolyte multilayers, the surface was rinsed using aqueous 0.15 M NaCl. All QCM-D measurements were performed under continuous flow condition with a flow rate of $50 \text{ } \mu\text{L min}^{-1}$.

The interactions of the polyelectrolyte multilayer films with different anions were studied using QCM-D. First, the PEM-modified QCM sensors mounted in the flow cells were exposed to Milli-Q water for one hour to remove residual NaCl used during the build-up. Then, the QCM-D signal was recorded for about 20 min, while still flushing with Milli-Q water to obtain the baseline. The 10 mM aqueous salt solutions were injected to the QCM-D cells, and the interactions with the multilayers were detected by the frequency shift and dissipation shift and interpreted by the mass change on the sensor surface. Finally, the salt solution was replaced by Milli-Q water and the signal was recorded.

The QCM frequency shifts (Δf) and dissipation shifts (ΔD) were acquired at the 3rd (15 MHz), 5th (25 MHz), 7th (35 MHz), 9th (45 MHz) and 11th (55 MHz) harmonic. With the help of the QTools software, the Voigt model was used to analyze the QCM-D data and calculate the adsorbed mass (thickness) of the soft and hydrated polyelectrolyte layers in liquid.^{48,49} Details regarding the modelling, including a validation of the obtained parameters are reported in the ESI† (Table S1). To determine the dry mass of the polyelectrolyte multilayers, the frequency response of the bare QCM sensors in air was firstly recorded as the base line, and then the frequency shift caused by the adsorption of polyelectrolyte multilayers onto sensor surfaces was determined after the multilayer build-up. To this end, the PEMs were rinsed with Milli-Q water and blow-dried in a stream of N₂ before subjecting them to the QCM-D measurement under ambient conditions. It is noted that this way residual water may be present, which would result in an overestimation of the dry mass. The ‘dry’ mass (thickness) of the polyelectrolyte multilayers adsorbed onto the sensor surfaces can be estimated from the decrease of the frequency of quartz crystal using Sauerbrey equation:⁵⁰

$$\Delta m = \frac{-c \times \Delta f_n}{n} \quad (2)$$

where Δm is the areal mass density of the adsorbed polyelectrolytes (ng cm^{-2}), Δf_n the frequency shift, c ($17.7 \text{ ng cm}^{-2} \text{ Hz}^{-1}$) the so-called mass-sensitivity constant, and n the harmonic number (3, 5, 7, 9, 11).

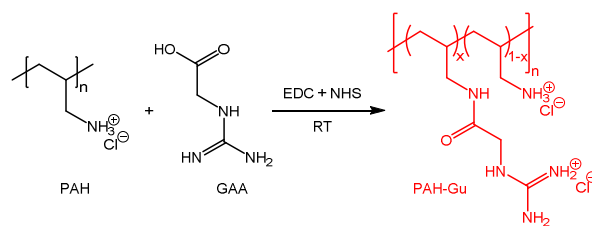
The thickness of the blow-dried PEM-coated QCM sensors was also determined by a variable-angle spectroscopic ellipsometer (VASE) VB-400 in the range of 400-1000 nm. The angle of incidence was varied between 74° and 76° in 1° steps. A Cauchy model implemented in the software package WVASE32 was employed to extract the optical thickness of the PEMs. The refractive index of the complete PEM was fixed at 1.45.⁵¹

After the QCM-D experiments, the PEM-coated QCM sensors were removed from the flow cell and characterized by Reflection Absorption Infrared spectroscopy (RAIR) under vacuum conditions (3 mbar) on a Bruker 66 V/S FT-IR spectrometer. A Mid-InfraRed (MIR) Deuterated TriGlycine Sulfate (DTGS) detector was used to collect the signal at a resolution of 3 cm^{-1} . A sample shutter accessory was mounted into the chamber for interleaved sample and background scanning. The infrared spectra of the polyelectrolyte multilayers were obtained at an angle of incidence of 70° with respect to the surface normal. A clean gold surface was measured as background prior to the measurements.

3 Results and discussion

3.1 Synthesis and characterization of PAH-Gu

A series of guanidinium-functionalized poly(allylamine hydrochlorides) (PAH-Gu) were synthesized by covalently attaching guanidine acetic acid (GAA) to PAH via a carbodiimide-assisted coupling reaction. This results in the formation of carbon amide bonds (-CO-NH-) and the introduction of guanidinium groups (Scheme 1).



Scheme 1 Schematic representation of the functionalization of poly(allylamine hydrochloride) (PAH) with guanidine acetic acid (GAA) at room temperature (RT). EDC and NHS stand for the coupling reagents N-(3-dimethylaminopropyl)-N'-ethylcarbodiimide hydrochloride and N-hydroxysuccinimide, respectively.

^1H NMR spectra of pure PAH, GAA, and the PAH-Gu polymers confirmed that the guanidinium groups were covalently attached to PAH chains (Fig. S1 and S2 in ESI †). The ^1H NMR spectrum of the synthesized PAH-Gu polymer (PAH-Gu #1) using a molar feed ratio of GAA: PAH = 1:10 shows a peak at 3.17 ppm, which is characteristic for the methylene protons next to the carbonyl moiety (Fig. S1 in ESI †). Note that in the ^1H NMR spectrum of GAA, this characteristic peak is located at 3.66 ppm (Fig. S2 in ESI †).^{52,53} The shift of this peak to higher field in the PAH-Gu indicates that the guanidine moiety is protonated. Upon increasing the molar feed ratio to 2:10 and 3:10, the intensity of this peak increases, indicating more covalently bound guanidinium groups. The degree of substitution (DS) as calculated from the ^1H NMR is listed in Table 1 for each molar feed ratio. While the obtained DS values of PAH-Gu #1 and PAH-Gu #3 are very much comparable to the feed ratio, the DS value for PAH-Gu #2 is 20% higher than theoretically can be expected. This is likely the result of the error made in the integration of the relatively small peak at 3.66 ppm, which appears as a shoulder of a much larger peak at a lower ppm value. This hampers an accurate quantification for the DS, but nevertheless the DS values follow the trend of the feed ratio.

Table 1 The degree of substitution and chemical yield as a function of molar feed ratio.

Sample	Feed ratio of GAA/ammonium (mol/mol)	Degree of substitution (DS) via ^1H NMR (%)	Chemical Yield, after dialysis (%)
PAH	0:10	-	-
PAH-Gu #1	1:10	9	~69
PAH-Gu #2	2:10	24	~68
PAH-Gu #3	3:10	29	~43

Given the uncertainty in the DS, the molecular weight of the synthesized PAH-Gu derivatives is not exactly known. Hence we calculated the chemical yield by dividing the mass of the product obtained after the dialysis by the sum of the masses of the starting compounds PAH and GAA. As each amide bond formation goes with the formation of a water molecule, the mass of the product—and hence the chemical yield—was slightly underestimated as we did not correct the mass for this. The thus-obtained yields were found to be in range of 43-69%.

The modification of PAH with GAA was also confirmed by the FT-IR (Fig. S3 in ESI†). The spectra of the non-functionalized PAH and the PAH-Gu polymers all show broad bands between 3200 and 3600 cm^{-1} , which are assigned to the anti-symmetric stretching mode of primary ammonium groups (Fig. S3a in ESI†).⁵⁴ The FT-IR spectra of PAH-Gu polymers #2 and #3 exhibit the characteristic peaks of the carbon amide groups at 1650 cm^{-1} (C=O stretching) and 1551 cm^{-1} (C-N stretching, N-H bending). These peaks are less visible in the case of PAH-Gu #1, which has the lowest DS. In the spectra of the PAH-Gu polyelectrolytes a band at $\sim 1650 \text{ cm}^{-1}$ is observed, which is assigned to the presence of $-\text{C}=\text{N}$ bonds in the guanidinium moiety. This value is lower than the associated band observed for pure GAA (1672 cm^{-1}).⁵⁵ This can be explained by presence of a proton, reducing the electron density of the C=N bond and hence the bond strength. This is in line with the observed methylene shift in ^1H NMR due to protonation.

In conclusion, both ^1H NMR and FT-IR measurements confirm that PAH-Gu polymers with various degrees of substitution were synthesized by changing the feed ratio of PAH and GAA. In the remaining of the study PAH-Gu #2 was used for the build-up of multilayer thin films on two different surfaces: SiO_2 -covered silicon surfaces and gold surfaces of QCM sensors.

3.2 PEM Build-up studied with reflectometry

Polyelectrolyte multilayers were (LbL) deposited on oxide-covered silicon wafers (hereafter called silica). First, analogue to related studies,^{23,56} a layer of polyethylenimine (PEI) was adsorbed, followed by the successive and alternate deposition of PSS and PAH or PAH-Gu from their solutions (concentration of 22 mg L^{-1} , 0.15 M NaCl and $\text{pH} = 5.5$). The layer build-up was studied by fixed-angle optical reflectometry in order to compare the process for using non-functionalized PAH and guanidinium-functionalized PAH-Gu. In Fig. 1a the real-time change in the reflection signal is shown for the build-up of PEMs with either PAH (blue in Fig. 1) or PAH-Gu (red in Fig. 1). After ~ 5 min of flushing with aqueous 0.15 M NaCl , the liquid is switched to an aqueous PEI solution (50 mg L^{-1}) containing 0.15 M NaCl . This resulted in a change of the $\Delta S/S_0$ values of $\sim 0.029 \pm 0.01$ and 0.038 ± 0.03 for the two analyzed samples (Fig. 1), corresponding to $\sim 0.69 \text{ mg m}^{-2}$ and $\sim 0.90 \text{ mg m}^{-2}$, respectively (as calculated by eqn (1)).

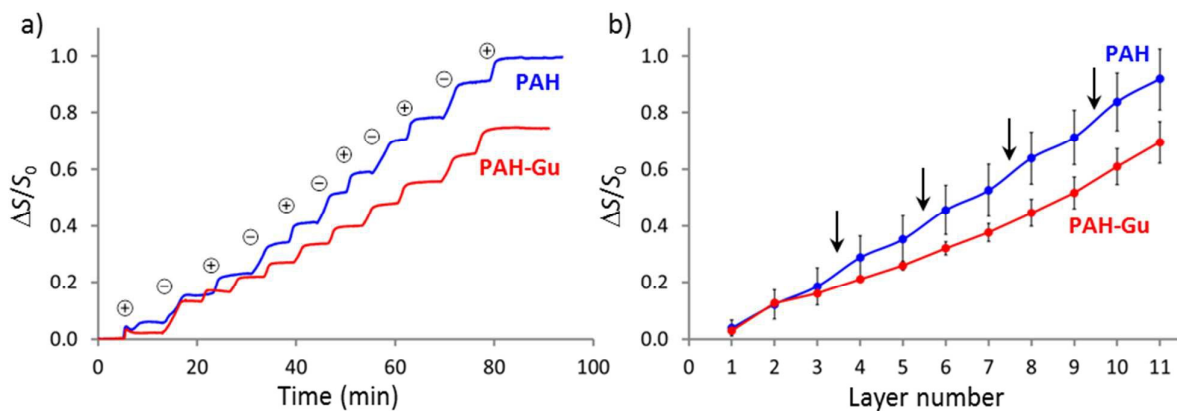


Fig. 1 a) Real-time change of $\Delta S/S_0$ for the build-up of PEI(PSS/PAH-Gu)₅ (labelled as PAH-Gu, red) and PEI(PSS/PAH)₅ (labelled as PAH, blue) PEMs in 0.15 M NaCl solutions at pH 5.5. b) Comparison of these two PEM systems as a function of layer number monitored in 0.15 M NaCl solutions at pH 5.5. The even numbers represent layers of PSS, while the odd numbers represent layers of the polycation used.

Using the same PEI concentration and almost the same pH value, Mészáros *et al.* obtained a value of $\sim 0.4 \text{ mg m}^{-2}$ at 0.01 M NaCl.⁵⁷ Our results at 0.15 M NaCl are in line with this, as the adsorbed amount of PEI onto silica was found to increase with increasing salt concentration.⁵⁸

After the successful adsorption of the first layer, the PEI solution was replaced by a PSS solution (22 mg L^{-1}) resulting in total changes of $\Delta S/S_0 = 0.13 \pm 0.01$ and 0.12 ± 0.05 for both bilayer build-ups. Then, a layer of PAH (or PAH-Gu) was deposited using a solution of 22 mg dm^{-3} of the respective polycation. These last two steps were repeated until (PSS/PAH)₅ and (PSS/PAH-Gu)₅ PEMs were built onto the PEI-covered silica surfaces. In Fig. 1b the observed stepwise increase of $\Delta S/S_0$, which is linearly related to the mass per area, is shown for both types of PEMs. The data shows for both systems a good (LbL) deposition. It is found that the Gu-containing PEM has a lower $\Delta S/S_0$ value compared to the Gu-free PEM (0.61 vs. 0.84). Unfortunately the dn/dc values are not known for all polymers, and likely they will vary to some extent. If they would be similar for the polymers used, our results would indicate

that about 27% less mass is deposited for the system using PAH-Gu. This difference must originate from the guanidinium functionality.

In an attempt to explain the observed difference we first consider potential differences in the charge density of the polycations. In a single-polymer-type solution at pH = 5.5, guanidinium ($pK_a \sim 13$) and the primary amines of PAH ($pK_a \sim 8.5$) will be fully protonated. While in solution the pK_a of a weak PE varies with the degree of ionization (due to effects of charge repulsion),⁵⁹ the apparent pK_a of PAH in a PAH/PSS multilayered system is larger than the one in solution.⁶⁰ Based on that we consider the differences in charge density to be marginal. Interestingly, Fig. 1b suggests that the overall difference between the two different types of PEM is mainly due to different amounts of PSS, particularly when the PEM has more than 3 PE layers. This is reflected by the different slopes of the PSS contributions in Fig. 1b (indicated by the arrows in Fig. 1b). In contrast, the slopes that are not marked by an arrow, which are associated to the adsorption of PAH or PAH-Gu, are nearly identical. In other words, the data suggests that less PSS adsorbs onto the PAH-Gu compared to PAH. This may be related to the attractive Gu-PSS interactions: in the case of the PSS/PAH-Gu PEM the PSS chains are more elongated ('flat'), while they are more coiled ('thicker') in PAH-containing PEMs. Remarkably, such behaviour is not observed when PAH or PAH-Gu adsorbed onto a PSS-terminated PEM. Finally, it is noted that the reasoning above only holds, when there is only a small or no difference in the dn/dc between the adsorbed polyelectrolytes.

Next, optical reflectometry was used to study the stability of PEMs with and without guanidinium at higher pH values. This is of special interest as the degree of protonation of PAH and PAH-Gu decreases upon increasing pH, resulting in a reduction of electrostatic interactions with the PSS, which might lead to destabilization of the PEMs. With pH 9 and 10 we have chosen two values above the pK_a of the primary amines, but low enough to avoid etching of the silica surface. Before the measurements, the multilayer-covered silica surfaces were submerged in Milli-Q water for one hour to remove any excess of NaCl from the

multilayers. The pH of the NaCl-free aqueous solutions was adjusted by the addition of aqueous 1 M NaOH solution before they were flushed through the flow cell. In Fig. 2 the reflectometry results are shown as relative changes of $\Delta S/S_0$ for the two PEM systems under study upon contacting the PEMs with aqueous solutions at pH 9 and 10.

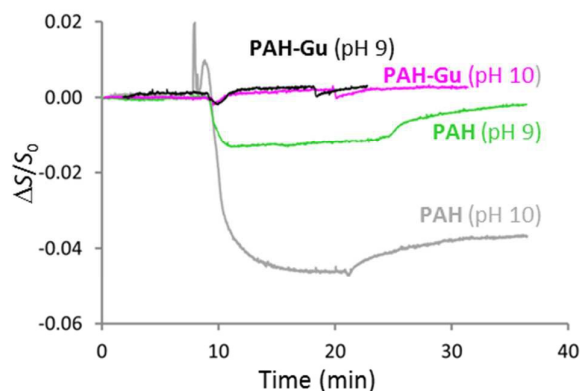


Fig. 2 Real-time $\Delta S/S_0$ signals PEMs built with PAH-Gu and PAH upon flushing with aqueous solutions at pH 9 and 10.

No significant change was observed for the Gu-containing PEM at both pH values, showing its high stability under these conditions. In contrast are the results obtained for the PEM that was made using (non-functionalized) PAH. At pH = 9, a decrease of $\Delta S/S_0 = 0.002$ is observed, indicating a loss of about 0.2%; and at pH = 10, $\Delta S/S_0 = 0.037$, reflecting a loss of 3.7% of mass. The obtained results are as expected and also in agreement with the results found by Dejeu *et al.*²⁰

3.3 PEM build-up studied with QCM-D

In addition to the work on reflectometry, the LbL deposition of PSS/PAH and PSS/PAH-Gu was investigated using QCM-D. The frequency response (here $\Delta f_3/3$), which is related to the

amount of adsorbed mass per area, and the dissipation response (here $\Delta D_3/3$), which is associated with the viscoelastic property of adsorbed layer, were monitored. This way we were able to follow the PEM formation by two different techniques that rely on very different principles (optical vs. mass). Moreover, QCM-D is of added value (to reflectometry) in terms of the viscoelastic properties. Typical QCM-D results are shown in Fig. 3. The QCM cell is first flushed with the NaCl solution (0.15 M, pH 5.5) to achieve a stable baseline, which serves as a reference for the subsequent measurements. Then (after at least 15 min), a PEI solution with a concentration of 50 mg dm^{-3} in 0.15 M NaCl (pH 5.5) is injected. Fig. 3a shows a decrease in the frequency shift after adding the PEI solution, indicating the adsorption of PEI chains onto the gold surfaces, which is in line with other studies.²⁵ After equilibrium was obtained, the solution was switched to the aqueous PSS solution to adsorb the next layer. The decrease in the frequency ($\Delta f_3/3$) and increase in dissipation ($\Delta D_3/3$, Fig. 3b) show that the polyelectrolytes deposit onto the surface. In addition, the dissipation shift of the PSS/PAH-Gu PEM is evidently lower than the one the PSS/PAH PEM. To facilitate the discussion of these results we present the QCM data as function of the layer number (Fig. 4).

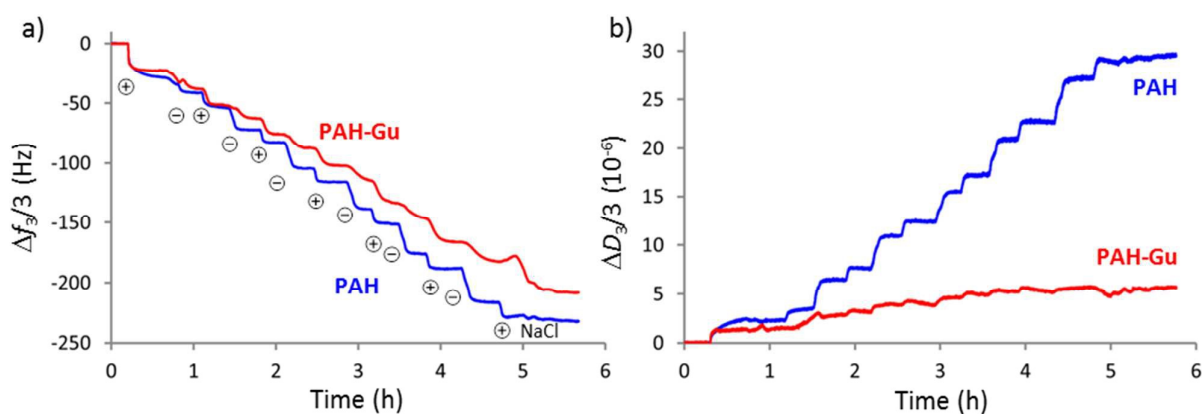


Fig. 3 Variation of the a) frequency shift ($\Delta f_3/3$) and b) dissipation shift ($\Delta D_3/3$) at the third harmonic for the build-up of PEMs made with PAH-Gu (red) and PAH (blue) in 0.15 M NaCl.

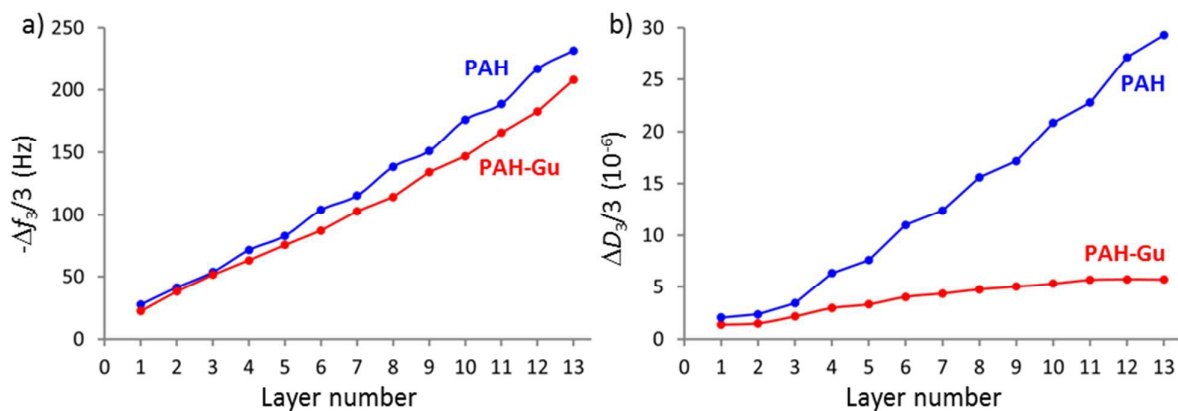


Fig. 4 The layer-number dependency of the a) frequency shift ($-\Delta f_3/3$) and b) dissipation shift ($\Delta D_3/3$) at the third harmonic for PEMs made with PAH-Gu and PAH, where the odd numbers represent the changes after the deposition of polycationic layers, while the even numbers represent the changes after the deposition of polyanionic layers.

Upon increasing the layer number, $-\Delta f_3/3$ increases, indicative for the sequential deposition of polyelectrolytes (Fig. 4a). It is found that the total frequency shift for the adsorption of PSS/PAH-Gu PEM is lower than that for the deposition of PSS/PAH PEM (207.93 vs. 231.56 Hz). Clearly the deposition of polyelectrolytes is affected by the type of the polycations, which is fully in line with the reflectometry results: compared to the PSS/PAH system, the use of PAH-Gu results in lower amounts of adsorbed material. This time this also includes the mass of associated water. Upon each addition of PSS, the change of $-\Delta f_3/3$ is larger when adsorbed onto a PAH-terminated PEM compared to PEM containing PAH-Gu as a top-layer. This observation is fully in line with the results of the optical reflectometer. While optical reflectometry shows hardly any difference between adding a layer of PAH or PAH-Gu onto a PSS-terminated PEM, QCM-D shows that the signal changes are larger upon additions of PAH-Gu, at least for layer numbers ≥ 8 . This may be the result of increased amounts of associated water, although guanidinium is known to be a weakly hydrated cation.⁶¹

Fig. 4b shows that the $\Delta D_3/3$ values gradually increase upon layer number increases. It is known that the dissipation change relates to the thickness and viscoelasticity of the PEMs on the QCM sensor surface. The relatively small change of $\Delta D_3/3$ observed in the adsorption of the PSS/PAH-Gu PEM also indicates that the use of PAH-Gu leads to a thinner, less viscoelastic and therefore more rigid multilayer, compared to the reference PSS/PAH PEM. By using the Voigt viscoelastic model,⁴⁸ the wet thickness of the hydrated PSS/PAH PEM in contact with an aqueous solution was calculated to be 53 nm, which is higher than the calculated value of 41 nm for the PSS/PAH-Gu PEM. In contrast, the ‘dry’ thicknesses of both blow-dried PEMs calculated by using the Sauerbrey equation were almost the same (32 and 34 nm, respectively), just like the optical thickness obtained by ellipsometry (22 and 23 nm, respectively). It is first noted that the differences between (and the accuracy of) the blow-dried, QCM-based thickness and the optical thickness may be related to assumptions made in the Sauerbrey and the optical model. Moreover, the presence of residual water overestimates the ‘dry’ thickness obtained with QCM and may also have affected the optical thickness. Indeed, the values of the optical thickness are lower and also the ratio between the wet and dry thickness is in line with literature.⁶² Data showing the reproducibility of the optical mass and a somewhat lower, but reasonable reproducibility of the wet mass, and hence the estimated water content is given in Table S2 of the ESI†.

In any case, the complete set of wet, blow-dried and optical thickness does indicate that different structures were formed in PAH and PAH-Gu multilayers during the deposition. In more detail, the largest changes in $\Delta D_3/3$ are found after the addition of a PSS layer onto a PAH- or PAH-Gu-terminated PEM. Furthermore, the changes in $\Delta D_3/3$ upon the addition of PAH are larger than those related to PAH-Gu. These observations support the picture we obtained from the optical reflectometry results: in PAH-containing PEMs the PSS chains are more coiled (i.e. less flat), which is in line with the larger PEM flexibility as observed with QCM-D.

To conclude this section, the PSS/PAH-Gu PEM shows a rigid and compact structure due to the presence of guanidinium groups on PAH-Gu chains, resulting in the strong electrostatic interactions between PAH-Gu and PSS chains with a relatively low amount of water molecules inside the multilayers. Compared to the PSS/PAH-Gu PEM, the PSS/PAH PEM has more highly hydrated and coiled polyelectrolyte chains, indicating more water molecules remaining in the multilayers.

3.4 Interaction of PEMs with anions

Next we studied the interaction between the PSS/PAH-Gu and PSS/PAH PEM systems and the salts by QCM-D. Fig. 5 presents the real-time frequency shifts ($\Delta f_3/3$) and dissipation shifts ($(\Delta D_3/3)$), recorded for both types of PEMs on QCM sensors exposed to different aqueous salt solutions, *i.e.* 10 mM of NaCl, NaNO₃, Na₂SO₄, and NaH₂PO₄, respectively. Both before and after exposure to the aqueous salt solutions, the QCM flow cell was rinsed with Milli-Q water. To facilitate a direct comparison between the different salts used, Fig. 6 summarizes the net frequency shifts ($\Delta f_3/3$) of the two PEM systems under study after the exposure to the different salt solutions, followed by flushing with Milli-Q water.

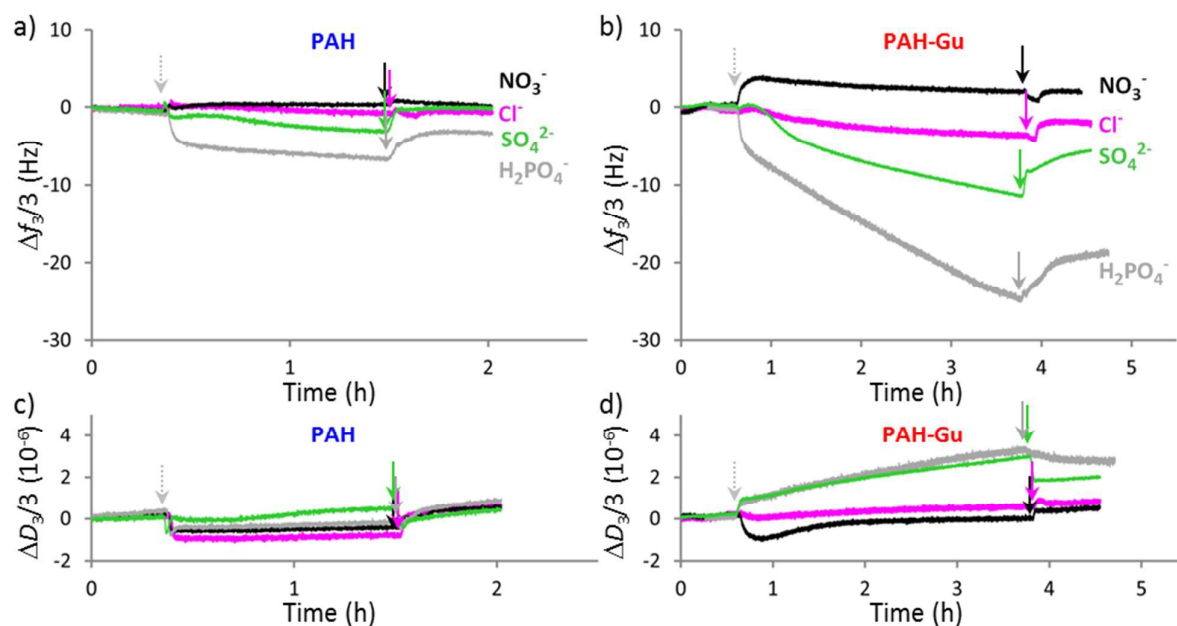


Fig. 5 The frequency shifts ($\Delta f_3/3$) and dissipation shift ($\Delta D_3/3$) at the third harmonic as a function of time, recorded for the PEM-modified QCM sensors exposed to different anion solutions containing 10 mM Cl^- (pink line), NO_3^- (black line), SO_4^{2-} (green line), and H_2PO_4^- (gray line), respectively. The dashed arrows indicate the moment in time at which the salt solutions were exposed to the QCM sensors; the arrows indicate the moment at which the solution was replaced by Milli-Q water again. Control QCM experiments showed that $\Delta f_3/3$ signals are hardly affected by the variation of solvent density and viscosity during solvent exchange (Fig. S4 in ESI†).

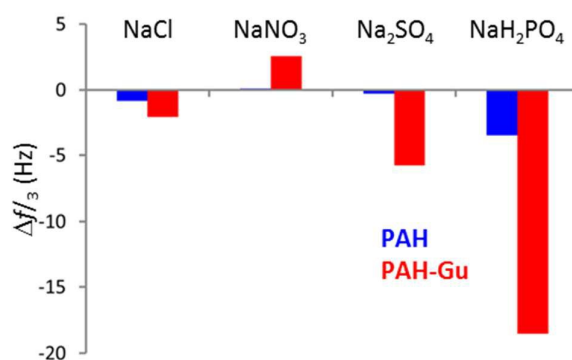


Fig. 6 The net frequency shifts ($\Delta f_3/3$) of the PEMs made with PAH and PAH-Gu on QCM sensors after the exposure to 10 mM aqueous solutions of NaCl, NaNO₃, Na₂SO₄ and NaH₂PO₄ and flushing with Milli-Q water.

In the case of the PAH PEM we observe that NaCl and NaNO₃ do not (or hardly) affect the frequency during flushing with salt (Fig. 5a). In the case of Na₂SO₄ and NaH₂PO₄ the frequency decreases slightly during the exposure to the salt solutions, indicating the swelling of the multilayers induced by the uptake of anions carrying hydrate water. After flushing with Milli-Q water the frequency recovers completely for Na₂SO₄, while in the case of NaH₂PO₄ an overall decrease of ~ 3.5 Hz is observed for $\Delta f_3/3$. This indicates that some H₂PO₄⁻ (and additional hydration water) is still present in the PEM, possibly as a result of replacing Cl⁻ as a counter ion of the ammonium groups on the PAH chains. Comparable observations have been reported by Zahn *et al.* in a QCM study on ferrocyanide-containing PEMs that were exposed to different salt solutions.²⁸

In order to have a more quantitative analysis we calculated the number of (water-free) H₂PO₄⁻ ions per unit area from the observed frequency shift using the Sauerbrey equation. The films do meet the commonly regarded criterion for rigid film, i.e. $\Delta Dn/(-\Delta fn/n) \ll 4 \times 10^{-7} \text{ Hz}^{-1}$,⁴⁹ validating the use of the Sauerbrey equation. Further it is noted that the mass of any associated water molecules is excluded from this calculation. Based on the differences in the molecular weight of H₂PO₄⁻ and Cl⁻, a shift of 3.5 Hz corresponds to a change of ~ 63 ng per nm², which equals to ~ 1.0 H₂PO₄⁻ anion per nm² (Table S3 in ESI†). The results of PSS/PAH-Gu PEM, however, show larger effects for all salts along the following trend: NaH₂PO₄ \gg Na₂SO₄ $>$ NaCl / NaNO₃ (Fig. 5b). Also, a brief, supportive RAIR study showed that the largest change in the region of 1400 to 1800 cm⁻¹ for the case where the Gu-containing PEM was exposed to NaH₂PO₄ (Fig. S6-S8 and Table S5 in ESI†). This order is

different than one would expect based on the Hofmeister series,⁶³ *i.e.* $\text{SO}_4^{2-} > \text{H}_2\text{PO}_4^- > \text{Cl}^- > \text{NO}_3^-$, which will be discussed in more detail below. In the case of NaH_2PO_4 the overall change in frequency shift was found to be ~ 18.50 Hz at the third harmonic, which corresponds to an areal density of $5.4 \text{ H}_2\text{PO}_4^-$ anions per nm^2 (water excluded). While the PEM layers did show some variation in the wet thickness, we attribute the additional response to the specific interaction between the guanidinium groups and H_2PO_4^- (Table S2 of the ESI†). As mentioned in the introduction, the guanidinium group is able to effectively capture phosphate anions by forming hydrogen bonds,³³ as *e.g.* applied in the development of a fluorescent sensor.⁶⁴ Compared to H_2PO_4^- , the adsorption of SO_4^{2-} leads to a relatively small frequency response of about 5.77 Hz, which is equal to an areal density of 1.7 SO_4^{2-} anions per nm^2 . The small amount of SO_4^{2-} anions binding to the PEM could be explained by its relatively high hydration energy, which is more than twice as high than the one of H_2PO_4^- ($-1080 \text{ kJ mol}^{-1}$ vs. -465 kJ mol^{-1} , Table S4 in ESI†). In other words, SO_4^{2-} is less likely to dehydrate, which results in fewer hydrogen bonds with guanidinium groups, leading to a relatively small amount of SO_4^{2-} binding with the multilayers. We remark that the Gu-functionalized multilayers show no obvious extra adsorption of Cl^- . The lower positive frequency change was observed when the multilayers were exposed to NO_3^- , indicating a slight shrinkage of the multilayers. This may be attributed to the affinity of NO_3^- to the film and the low extent of hydration of this anion (Table S4 in ESI†), resulting in dehydration, which is consistent with literature.²¹ Apart from the stronger PAH-Gu/ H_2PO_4^- interactions (compared to PAH-Gu/ SO_4^{2-}) there may also be an additional effect of the ion valency. After all, studies on the ion separation behavior of PEMs have shown that multivalent ions are more easily rejected than monovalent ions, partly due to electrostatic repulsion from the counter-charged parts of the PEM.^{9,65}

It is noted that the pH values of the non-phosphate salts are very close to each other (pH \sim 6), while the one of NaH_2PO_4 was found to be slightly lower (pH \sim 5). However, we did not correct the pH value as some divalent HPO_4^{2-} would be present as well at pH \sim 6. A control experiment showed that the frequency of PEM-modified QCM-D sensors was hardly affected upon changing the pH from 6 to 5 (Fig. S5 in ESI†).

Next, the dissipation shift recorded by QCM-D can provide additional information on (changes in) the structure and viscoelastic properties of thin layers deposited on the quartz crystals. The dissipation of the sensor with the PAH PEM increases gradually to a positive value upon the exposure to solutions of NaH_2PO_4 and NaSO_4 (Fig. 5d). After rinsing with Milli-Q water, both dissipation values decreased, but remained at more positive values than the initial ones. This is different from the experiments performed in aqueous solution of NaCl and NaNO_3 , where the dissipation shifts experienced a slight fluctuation at first, to finally reach a lower value after rinsing with Milli-Q water. The latter is also observed for PAH-based PEM and in this case the dissipation responses for NaH_2PO_4 and NaSO_4 are very much comparable (Fig. 5c).

To conclude this section, the high dissipation shift for NaH_2PO_4 observed for the guanidinium-functionalized PEMs can be explained by the strong interactions between H_2PO_4^- anions and the guanidinium groups. As reported in the literature,⁶⁶ two oxygen atoms of H_2PO_4^- form hydrogen bonds with the NH protons of guanidinium groups. As the H_2PO_4^- is not completely dehydrated and still carries water molecules, this results in the hydrated structures.

Conclusions

Poly(allylamine hydrochloride) derivatives containing guanidinium groups were successfully synthesized by a one-pot reaction using EDC/NHS chemistry. Optical reflectometry and

QCM-D measurements indicated that the newly synthesized PAH-Gu polymers can be used for building up PEMs on silica and Au surfaces. Compared to the guanidinium-free PEI(PSS/PAH)_n reference PEMs the resulting PEI(PSS/PAH-Gu)_n (n = 5 or 6) PEMs were found to i) contain less deposited material, ii) have a small wet thickness and, iii) be more rigid, iv) have a higher stability at high pH. The reflectometry data suggests that, compared to PAH, lower amounts of PSS are adsorbed onto PAH-Gu layers, which is indeed in line with the observed differences. We believe that this is due to the additional Gu-sulfonate interactions between PAH-Gu and PSS. Consequently, PSS may have a more elongated conformation upon adsorbing onto a PAH-Gu-terminated PEM.

Upon the exposure of a PAH-containing PEM to aqueous solutions of sodium salts it was shown with QCM-D that H₂PO₄⁻ was bound to the PEM, while this was hardly the case for SO₄²⁻, Cl⁻ and NO₃⁻. For PEMs built with the Gu-modified PAH the amount of bound H₂PO₄⁻ increased by a factor of 5 and also some SO₄²⁻ was bound. Also these differences can be understood by the presence of guanidinium, which is known to bind oxoanions. Due to its higher hydration energy, SO₄²⁻ bound less to the PSS/PAH PEMs compared to H₂PO₄⁻. Moreover, SO₄²⁻ may be repelled electrostatically to a higher extent due to its bivalency.

Finally, guanidinium-functionalized polyelectrolytes are able to favourably exchange H₂PO₄⁻, which is of possible benefit for the development of H₂PO₄⁻ sensors and ion separation /recovery systems based on PEMs.

Acknowledgements

This work was performed in the cooperation framework of Wetsus – European centre of excellence for sustainable water technology (www.wetsus.nl). Wetsus is funded by the Dutch Ministry of Economic Affairs and the Ministry of Infrastructure and Environment. The authors like to thank the participants of the research theme Biomimetic Membranes for the

fruitful discussions and their financial support. Dr. Wolter Jager and Mr. Lars van der Mee (both TU Delft, The Netherlands) are thanked for their support on the synthesis of PAH-Gu. Mr. Duco Bosma and Mr. Richard van Ravesloot (both TU Delft, The Netherlands) are thanked for their help on initial optical reflectometry measurements. Mr. Wuyuan Zhang (TU Delft, The Netherlands) is acknowledged for his help with freeze-drying. Mr. Remco Fokink (Wageningen University, The Netherlands) is acknowledged for growing the silica layers.

References

- 1 G. Decher, G. *Science*, 1997, **277**, 1232.
- 2 G. Decher and J. B. Schlenoff, *Multilayer Thin Films: Sequential Assembly of Nanocomposite Materials*, 2nd Edition, Wiley-VCH Verlag & Co. KGaA, Weinheim, Germany, 2012.
- 3 N. Joseph, P. Ahmadiannamini, R. Hoogenboom and I. F. J. Vankelecom, *Polym. Chem.*, 2014, **5**, 1817.
- 4 B. G. De Geest, C. Déjugnat, G. B. Sukhorukov, K. Braeckmans, S. C. De Smedt and J. Demeester, *Adv. Mater.*, 2005, **17**, 2357.
- 5 X. Zhang, H. Wang and Z. Su, *Langmuir*, 2012, **28**, 15705.
- 6 S. Pavlukhina, Y. Lu, A. Patimetha, M. Libera and S. Sukhishvili, *Biomacromolecules* 2010, **11**, 3448.
- 7 D. V. Andreeva, E. V. Skorb and D. G. Shchukin, *ACS Appl. Mater. Interfaces*, 2010, **2**, 1954.
- 8 A. Mentbayeva, A. Ospanova, Z. Tashmuhambetova, V. Sokolova and S. Sukhishvili, *Langmuir*, 2012, **28**, 11948.
- 9 G. Z. Garyfallou, L. C. P. M. de Smet and E. J. R. Sudhölter, *Sens. Actuators B: Chem.*, 2012, **168**, 207.
- 10 P.-G. Su and K.-H. Cheng, *Sens. Actuators B: Chem.*, 2009, **142**, 123.
- 11 I. Shazia, J. de Groot, K. Nijmeijer and W. M. Vos, *J. Colloid Interface Sci.*, 2015, **446**, 386.
- 12 R. Femmer, A. Mani and M. Wessling, *Sci. Rep.*, 2015, **5**, 11583.
- 13 S. Abdu, M.-C. Martí-Calatayud, J. E. Wong, M. García-Gabaldón and M. Wessling, *ACS Appl. Mater. Inter.*, 2014, **6**, 1843.
- 14 J. A. Armstrong, E. E. L. Bernal, A. Yaroshchuk and M. L. Bruening, *Langmuir*, 2013, **29**, 10287.
- 15 S. U. Hong, L. Ouyang, M. L. Bruening, *J. Membrane Sci.*, 2009, **327**, 2.
- 16 J. de Groot, R. Oborný, J. Potreck, K. Nijmeijer and W. M. de Vos, *J. Membrane Sci.*, 2015, **475**, 311.
- 17 A. Toutianoush, J. Schnepf, A. El Hashani and B. Tieke, *Adv. Funct. Mater.*, 2005, **15**, 700.
- 18 A. M. Balachandra, J. Dai and M. L. Bruening, *Macromolecules*, 2002, **35**, 3171.
- 19 I. Welterlich and B. Tieke, *Macromolecules*, 2011, **44**, 4194.
- 20 J. Dejeu, S. Diziain, C. Dange, F. Membrey, D. Charrat and A. Foissy, *Langmuir*, 2008, **24**, 3090.
- 21 M. Salomäki and J. Kankare, *Macromolecules*, 2008, **41**, 4423.
- 22 D. Yoo, S. S. Shiratori and M. F. Rubner, *Macromolecules*, 1998, **31**, 4309.
- 23 J. H. Choi, S.O. Kim, E. Linary, E. C. Dreaden, V. P. Zhdanov, P. T. Hammond and N.-J. Cho, *J Phys Chem B.*, 2015, **119**, 10554.
- 24 W. J. Dressick, K. J. Wahl, N. D. Bassim, R. M. Stroud and D. Y. Petrovykh, *Langmuir*, 2012, **28**, 15831.
- 25 G. Liu, Y. Hou, X. Xiao and G. Zhang, *J. Phys. Chem. B*, 2010, **114**, 9987.
- 26 A. E. El Haitami, D. Martel, V. Ball, H. C. Nguyen, E. Gonthier, P. Labbé, J.-C. Voegel, P. Schaaf, B. Senger and F. Boulmedais, *Langmuir*, 2009, **25**, 2282.
- 27 R. Steitz, W. Jaeger and R. v. Klitzing, *Langmuir*, 2001, **17**, 4471.
- 28 R. Zahn, F. Boulmedais, J. Vörös, P. Schaaf and T. Zambelli, *J. Phys. Chem. B*, 2010, **114**, 3759.
- 29 L. Wang, Y. Lin and Z. Su, *Soft Matter*, 2009, **5**, 2072.
- 30 D. Ullien, P. J. Harmsma, S. M. C. Abdulla, B. M. de Boer, D. Bosma, E. J. R. Sudhölter, L. C. P. M. de Smet and W. F. Jager, *Optics Express*, 2014, **22**, 16585.

- 31 L. van der Mee, E. S. Y. Chow, L. C. P. M. de Smet, M. de Puit, E. J. R. Sudhölter and W. F., *Anal. Methods*, in press.
- 32 X. Zhu, J. Yang and K. S. Schanze, *Photoch. Photobio. Sci.*, 2014, **13**, 293.
- 33 P. Blondeau, M. Segura, R. Perez-Fernandez and J. de Mendoza, *Chem. Soc. Rev.*, 2007, **36**, 198.
- 34 Z.-G. Wang, N. Lv, W.-Z. Bi, J.-L. Zhang and J.-Z. Ni, *ACS Appl. Matter: Inter.*, 2015, **7**, 8377.
- 35 W. N. George, M. Giles, I. McCulloch, J. H. G. Steinke and J. C. deMello, *ChemPhysChem*, 2011, **12**, 765.
- 36 G. Zhang and C. Wu, *Macromol. Rapid Commun.*, 2009, **30**, 328.
- 37 L. Fu, X. Chen, J. He, C. Xiong and H. Ma, *Langmuir*, 2008, **24**, 6100.
- 38 F. Höök, B. Kasemo, T. Nylander, C. Fant, K. Sott and H. Elwing, *Anal. Chem.*, 2001, **73**, 5796.
- 39 Z. Cao, T. Tsoufis, T. Svaldo-Lanero, A.-S. Duwez, P. Rudolf and K. Loos, *Biomacromolecules*, 2013, **14**, 3713.
- 40 B.-Y. Du, X. Fan, Z. Cao and X.-L. Guo, *Chin. J. Anal. Chem.*, 2010, **38**, 752.
- 41 Z. Cao, B. Du, T. Chen, H. Li, J. Xu and Z. Fan, *Langmuir*, 2008, **24**, 5543.
- 42 B. Du and D. Johannsmann, *Langmuir*, 2004, **20**, 2809.
- 43 R. Zahn, K. R. Bickel, T. Zambelli, J. Reichenbach, F. M. Kuhn, J. Vörös, R. Schuster, *Soft Matter*, 2014, **10**, 688.
- 44 L. Shen, P. Chaudouet, J. Ji, C. Picart, *Biomacromolecules*, 2011, **12**, 1322.
- 45 W.-B. Tsai, C.-Y. Chien, H. Thissen and J.-Y. Lai, *Acta Biomater.*, 2011, **7**, 2518.
- 46 J. C. Dijt, M. A. C. Stuart and G. J. Fleer, *Adv. Colloid Interface Sci.*, 1994, **50**, 79.
- 47 L. Lee, A. P. R. Johnston and F. Caruso, *Biomacromolecules*, 2008, **9**, 3070.
- 48 M. Rodahl, F. Höök, C. Fredriksson, C. A. Keller, A. Krozer, P. Brzezinski, M. Voinova and B. Kasemo, *Faraday Discuss.*, 1997, **107**, 229.
- 49 D. Reviakine, D. Johannsmann and R. P. Richter, *Anal. Chem.*, 2011, **83**, 8838.
- 50 G. Sauerbrey, *Z. Phys.*, 1959, **155**, 206.
- 51 Z. Feldötö, I. Varga and E. Blomberg, *Langmuir* 2010, **26**, 17048.
- 52 U. F. H. Engelke, M. Tassini, J. Hayek, M. de Vries, A. Bilos, A. Vivi, G. Valensin, S. Buoni, R. Zannolli, W. Brussel, B. Kremer, G. S. Salomons, M. J. B. M. Veendrick-Meeke, L. A. J. Kluijtmans, É. Morava and R. A. Wevers, *NMR Biomed.*, 2009, **22**, 538.
- 53 J. L. de Miranda, J. da Silva Coelho, L. C. de Moura, M. H. Herbst, B. A. C. Horta, R. B. de Alencastro and M. G. Albuquerque, *Polyhedron*, 2008, **27**, 2386.
- 54 F. Tristán, G. Palestino, J. L. Menchaca, E. Pérez, H. Atmani, F. Cuisinier and G. Ladam, *Biomacromolecules*, 2009, **10**, 2275.
- 55 J. L. de Miranda and J. Felcman, *Synth. React. Inorg. Met.-Org. Chem.*, 2001, **31**, 873.
- 56 E. Poptoshev, B. Schoeler and F. Caruso, *Langmuir*, 2004, **20**, 829.
- 57 R. Mészáros, I. Varga and T. Gilányi, *Langmuir*, 2004, **20**, 5026.
- 58 R. Mészáros, L. Thompson, M. Bos and P. de Groot, *Langmuir*, 2002, **18**, 6164.
- 59 S. W. Cranford, C. Ortiz and M. J. Buehler, *Soft Matter*, 2010, **6**, 4175.
- 60 A. I. Petrov, A. A. Antipov and G. B. Sukhorukov, *Macromolecules*, 2003, **36**, 10079
- 61 P. E. Mason, G. W. Neilson, C. E. Dempsey, A. C. Barnes and J. M. Cruickshank *Proc. Natl. Acad. Sci.* 2004, **100**, 4557.
- 62 M. Porus, P. Maroni and M. Borkovec, *Langmuir*, 2012, **28**, 5642.
- 63 F. Hofmeister, *Arch. Exp. Pathol. Pharmacol.*, 1888, **24**, 247.
- 64 I. Tabujew, C. Freidel, B. Krieg, M. Helm, K. Koynov, K. Müllen and K. Peneva, *Macromol. Rapid Comm.*, 2014, **35**, 1191.
- 65 B. Tieke and A. Toutianoush, W. Jin, *Adv. Colloid Interface Sci.*, 2005, **116**, 121.
- 66 F. A. Cotton, V. W. Day, E. E. Hazen and S. Larsen, *J. Am. Chem. Soc.*, 1973, **95**, 4834.

Guanidinium-functionalized polyelectrolyte multilayers absorb more H_2PO_4^- compared to other anions and to polyelectrolyte multilayers without guanidinium.

